



Impact of Superthermal Electrons in the Mars' lower Ionosphere

N. A. Asal^{1,*}, I. S. Elkamash², M. El-Metwally¹, and W. M. Mosleml^{1,3}

¹ Department of Physics, Faculty of Science, Port Said University, Port Said 42521, Egypt.

² Department of Physics, Faculty of Science, Mansoura University, Mansoura 35516, Egypt

³ Centre for Theoretical Physics, The British University in Egypt (BUE), El-Shorouk City, Cairo, Egypt.

*Corresponding author: nourasl44@gmail.com

ABSTRACT

Recent research has increasingly focused on understanding ion escape from Mars' ionosphere, a phenomenon that contributes significantly to atmospheric loss. Various models have emerged to explain the escape of charged particles from the Martian atmosphere, with one prominent explanation being the plasma expansion approach. This model suggests that the ionosphere undergoes continuous ion loss, with hundreds of tons of ions escaping daily. A key factor in this process is the presence of superthermal electrons in the lower Martian ionosphere, which have been observed to play a crucial role in enhancing plasma dynamics. The ionosphere of Mars is composed of three main positive ion species O_2^+ , O^+ and CO_2^+ , accompanied by superthermal electrons, forming a complex plasma system. To investigate the ion loss processes, we model this system using a set of hydrodynamic fluid equations, incorporating the effects of superthermal electrons. The equations are reduced using a self-similar transformation, simplifying the problem into a set of ordinary differential equations. These equations are solved numerically to determine the plasma expansion characteristics, including ion density, velocity, and electric potential. Our study reveals the significant influence of superthermal electrons on plasma expansion, highlighting their role in enhancing ion escape and altering the plasma behavior. This approach provides new insights into the complex interactions within the Martian ionosphere and contributes to our understanding of atmospheric evolution on Mars.

Keywords: Mars ionosphere; Plasma expansion; Low altitude; Superthermal electrons.

1. INTRODUCTION

Mars is the closest planet to Earth and fourth in distance from the Sun in our solar system. The atmosphere of the terrestrial planet Mars is thin and consists of about 95% CO_2 . The dynamics and

chemistry in Mars' surrounding atmosphere impact its plasma environment. The Martian upper atmosphere is directly exposed to the solar wind since atoms are removed from the outer layer without a global magnetic field like Venus [1]. Many missions to Mars have been launched such as Mars Global Surveyor, Vikings, Phobos, and Mars Express, among others. Only four of the forty space missions, or ten percent of the total number of missions, contained equipment capable of detecting and observe plasma. NASA initiated the Mars Atmosphere and Volatile Evolution (MAVEN) mission in 2013 with the primary objective of evaluating the state of Mars' upper atmosphere at the present time while investigating the various processes that impact it [2]. Based on measurements from MAVEN at altitudes between 180 and 500 km, it was observed that the lower ionosphere of Mars is dominated by the ions O_2^+ , O^+ and CO_2^+ [3-5]. These ions are considered to be a significant component of the Martian ionosphere [6-7], superthermal electrons have been observed in Mars [8-9].

The disappearance of Mars' global magnetic field approximately 4 billion years ago, along with the evolution of the Sun, has played a significant role in the atmospheric dynamics of the planet [10]. Without the protection of a global magnetic field, the upper atmosphere of Mars directly interacts with the solar wind, allowing continuous atmospheric ion escape. These ions escape through two major outflow mechanisms: one being a cold, fluid-like outflow extending into the tail region, and the other, a more energetic flow driven by the convective electric field created through the interaction between the solar wind and the Martian ionosphere. The latter forms the so-called "Martian ion plume." This process of ion loss is driven by plasma expansion and involves charge separation. When lighter electrons accelerate first, an ambipolar electric field develops that pulls ions along to maintain quasi-neutrality [11].

The superthermal electron distribution is represented by the kappa distribution (κ), which is also found in many space plasma environments. This distribution has been applied for the analysis and interpretation of observational data from various systems, such as Earth's magnetosphere [12], the solar wind [13], and the magnetospheres of Jupiter and Saturn [14]. In general, the κ parameter effectively indicates the deviation from a Maxwellian distribution. A smaller value of κ suggests a system that is significantly deviated from Maxwellian distribution, where some electrons gain higher energy than predicted. Larger values of κ indicate a return to the dominance of the Maxwellian distribution [15-16].

The study by Moslem and El-Said [17] examined nano-structure formation on quartz surfaces induced by slow, highly charged ions. It concluded that increases in temperature within the plasma region lead to the formation of taller nano-hillocks as a result of plasma expansion. This process is influenced by the presence of nano-dust particles. Elkamash and Kourakis [18] addressed multispecies plasma expansion by using a two-ion fluid model, which demonstrated the strong energization of suprathermal electrons at the expansion front, enhancing ion acceleration. Salem and El-Labany [19] also investigated ion escape from Titan's ionosphere and found that solar wind electrons promote ion loss, with heavier ions playing a more significant role in this process. Finally, Salem and Lazar [20] explored the role of the solar wind in the upper ionosphere of Venus, illustrating how its key parameters, particularly density and temperature, control ion acceleration and outflow. Together, these complementary studies provide a comprehensive understanding of plasma expansion both in planetary atmospheres and laboratory plasmas.

In this paper, a multi-fluid hydrodynamic model is used to describe the plasma. It considers three positive ion species O_2^+ , O^+ and CO_2^+ , along with the superthermal electron population. In the next section, the hydrodynamic fluid equations will be presented, along with the formulation of the theoretical model adopted. Section 3 is devoted to the numerical results and discussion, while Section 4 summarizes the most important conclusions of the paper.

2. FORMULATION OF THEORETICAL MODEL

We consider the plasma model to be a collisionless, unmagnetized cold plasma composed of three positive ion species O_2^+ , O^+ and CO_2^+ and a superthermal electron distribution.

For O_2^+ ,

$$\frac{\partial n_{O_2}}{\partial t} + \frac{\partial}{\partial x} n_{O_2} u_{O_2} = 0, \quad (1)$$

$$n_{O_2} m_{O_2} \left(\frac{\partial u_{O_2}}{\partial t} + u_{O_2} \frac{\partial u_{O_2}}{\partial x} \right) + e n_{O_2} \frac{\partial \phi}{\partial x} = 0, \quad (2)$$

for O^+ ,

$$\frac{\partial n_O}{\partial t} + \frac{\partial}{\partial x} n_O u_O = 0, \quad (3)$$

$$n_O m_O \left(\frac{\partial u_O}{\partial t} + u_O \frac{\partial u_O}{\partial x} \right) + e n_O \frac{\partial \phi}{\partial x} = 0, \quad (4)$$

for CO_2^+ ,

$$\frac{\partial n_{CO_2}}{\partial t} + \frac{\partial}{\partial x} n_{CO_2} u_{CO_2} = 0, \quad (5)$$

$$n_{CO_2} m_{CO_2} \left(\frac{\partial u_{CO_2}}{\partial t} + u_{CO_2} \frac{\partial u_{CO_2}}{\partial x} \right) + e n_{CO_2} \frac{\partial \phi}{\partial x} = 0, \quad (6)$$

for superthermal electrons,

$$n_e = n_{e0} \left(1 - \frac{\left(\frac{e \phi}{k_B T_e} \right)^{\left(\frac{1}{2} - \kappa \right)}}{\left(\kappa - \frac{3}{2} \right)} \right). \quad (7)$$

The equations (1) – (7) are supplemented by the plasma neutrality condition, which is expressed as follows:

$$n_{O_2} + n_O + n_{CO_2} - n_e = 0. \quad (8)$$

Here is the revised version of your paragraph with improved clarity, grammar, and punctuation:

From Eq. (8), the quasi-neutrality condition has been widely demonstrated to be a good approximation for studies of plasma in short wave-numbers or systems with very small Debye lengths. It is found that the plasma scale is much larger compared to the Debye length, thus ensuring the validity of the quasi-neutrality approximation. However, if the plasma scale is comparable to or larger than the Debye length, a plasma sheath forms near the boundary. In this case, no self-similar solution can be obtained using the Poisson equation. Therefore, we use the plasma approximation to solve the basic equations and perform a quantitative analysis of the problem [21].

The symbols n_j , u_j and ϕ refer to densities, velocities, and electric potential, respectively, where $j = O_2, O, CO_2$ and e . T_e is the constant temperature of the superthermal electron with mass m_j . Note that our study is a local analysis, and to satisfy the condition of self-similarity we assume that the temperature is constant. In this context, where partial differentiation is not easily applicable, a self-similar transformation is used to reduce the partial differential equations to ordinary differential equations. These ordinary equations are more manageable and easier to interpret for plasma expansion. It is important to note that a self-similar numerical solution corresponds to the asymptotic behavior of an unbounded plasma system. However, using such a transformation inherently leads to a loss of information regarding characteristic lengths and times. We succeeded in characterizing the expanding plasma in the co-moving frame, using a velocity specified by the ion acoustic speed $C_s = (k_B T_e / m_{O_2})^{1/2}$. This approach is widely employed in research to investigate various processes occurring in laboratory plasmas [11,22,23], space plasmas [19,24,25], surface nano-structure creation [17], laser-plasma interactions [26-27], and the dynamics of astrophysical objects [18-28]. To solve Eqs. (1)–(8), This approach requires introducing a new variable $\xi = x / (C_s t)$ [29,30] obtain the following normalized ordinary differential equations:

$$(V_{O_2} - \xi) \frac{\partial N_{O_2}}{\partial \xi} + N_{O_2} \frac{\partial V_{O_2}}{\partial \xi} = 0, \tag{9}$$

$$(V_{O_2} - \xi) \frac{\partial V_{O_2}}{\partial \xi} + \frac{\partial \Phi}{\partial \xi} = 0, \tag{10}$$

$$(V_0 - \xi) \frac{\partial N_0}{\partial \xi} + N_0 \frac{\partial V_0}{\partial \xi} = 0, \tag{11}$$

$$(V_0 - \xi) \frac{\partial V_0}{\partial \xi} + Q_0 \frac{\partial \Phi}{\partial \xi} = 0, \tag{12}$$

$$(V_{CO_2} - \xi) \frac{\partial N_{CO_2}}{\partial \xi} + N_{CO_2} \frac{\partial V_{CO_2}}{\partial \xi} = 0, \tag{13}$$

$$(V_{CO_2} - \xi) \frac{\partial V_{CO_2}}{\partial \xi} + Q_{CO_2} \frac{\partial \Phi}{\partial \xi} = 0, \tag{14}$$

$$\frac{1}{N_e} \frac{\partial N_e}{\partial \xi} - \frac{(\kappa - \frac{1}{2})}{(\kappa - \frac{3}{2} - \Phi)} \frac{\partial \Phi}{\partial \xi} = 0, \tag{15}$$

$$\alpha \frac{\partial N_{O_2}}{\partial \xi} + \beta \frac{\partial N_0}{\partial \xi} + \gamma \frac{\partial N_{CO_2}}{\partial \xi} - \frac{\partial N_e}{\partial \xi} = 0. \tag{16}$$

In Eqs. (9)–(16), we have used the following ratio $Q_0 = m_{O_2}/m_0, Q_{CO_2} = m_{O_2}/m_{CO_2}$, $\alpha = n_{O_{2_0}}/n_{e_0}$, $\beta = n_{O_0}/n_{e_0}$ and $\gamma = n_{CO_{2_0}}/n_{e_0}$ where $n_{O_{2_0}}, n_{O_0}, n_{CO_{2_0}}$ and n_{e_0} are the initial densities of the plasma species, N_{O_2, O, CO_2} are the normalized density by the unperturbed density $n_{O_{2_0}}, n_{O_0}, n_{CO_{2_0}}$ and n_{e_0} . V_{O_2, O, CO_2} is the normalized velocity by the ion-acoustic speed $C_s = (k_B T_e / m_{O_2})^{1/2}$ and Φ is the normalized potential by $k_B T_e / e$.

We conduct a numerical analysis to investigate the characteristics of plasma expansion profiles for both cases O_2^+ and O^+ , as well as CO_2^+ ions. Equations (9) – (16) can be rewritten in a matrix form as follows:

$$\begin{pmatrix} (V_0 - \xi) & N_0 & 0 & 0 & 0 & 0 & 0 & 0 & 0 \\ 0 & (V_0 - \xi) & 0 & 0 & 0 & 0 & 0 & 0 & Q_0 \\ 0 & 0 & (V_{O_2} - \xi) & N_{O_2} & 0 & 0 & 0 & 0 & 0 \\ 0 & 0 & 0 & (V_{O_2} - \xi) & 0 & 0 & 0 & 0 & 1 \\ 0 & 0 & 0 & 0 & (V_{CO_2} - \xi) & 0 & 0 & 0 & 0 \\ 0 & 0 & 0 & 0 & 0 & N_{CO_2} & 0 & 0 & Q_{CO_2} \\ 0 & 0 & 0 & 0 & 0 & (V_{CO_2} - \xi) & 0 & 0 & 0 \\ \beta & 0 & \alpha & 0 & \gamma & 0 & \frac{1}{N_e} & \frac{(\kappa - \frac{1}{2})}{(\kappa - \frac{3}{2} - \Phi)} & 0 \end{pmatrix} \times \begin{pmatrix} N_0' \\ V_0' \\ N_{O_2}' \\ V_{O_2}' \\ N_{CO_2}' \\ V_{CO_2}' \\ N_e' \\ \Phi' \end{pmatrix} = 0. \tag{17}$$

The prime indicates the first derivative in variable ξ . To solve the basic equations numerically, we need a nontrivial solution which is obtained when the following determinant vanishes:

$$\begin{vmatrix}
 (V_0 - \xi) & N_0 & 0 & 0 & 0 & 0 & 0 & 0 \\
 0 & (V_0 - \xi) & 0 & 0 & 0 & 0 & 0 & Q_0 \\
 0 & 0 & (V_{O_2} - \xi) & N_{O_2} & 0 & 0 & 0 & 0 \\
 0 & 0 & 0 & (V_{O_2} - \xi) & 0 & 0 & 0 & 1 \\
 0 & 0 & 0 & 0 & (V_{CO_2} - \xi) & N_{CO_2} & 0 & 0 \\
 0 & 0 & 0 & 0 & 0 & (V_{CO_2} - \xi) & 0 & Q_{CO_2} \\
 0 & 0 & 0 & 0 & 0 & 0 & \frac{1}{N_e} & \frac{\kappa - \frac{1}{2}}{\kappa - \frac{3}{2} \Phi} \\
 \beta & 0 & \alpha & 0 & \gamma & 0 & -1 & 0
 \end{vmatrix} = 0. \quad (18)$$

We use appropriate numerical Mathematica code to solve this determinant and select a positive solution for V_{O_2} , which refers to the plasma expanding in $+\xi$, and then Eqs. (9)–(16) can be solved numerically. We solved a set of hydrodynamic fluid equations describing plasma expansion by the self-similar approach. In the self-similar method, space and time combine into one dimensionless variable ξ , representing space and time with respect to the physical properties of plasma, such as ion-acoustic speed C_s plasma Debye length λ_{De} , and the inverse of the plasma frequency ω_e^{-1} .

3. NUMERICAL RESULTS AND DISCUSSION

We are motivated by the data obtained from MAVEN, we used the ionospheric data for the O_2^+ , O^+ and CO_2^+ number densities (10^9 – 10^{10}), (10^9 – 10^{11}) and (10^6 – 10^9) m^{-3} , respectively. Also, we used the O_2^+ , O^+ and CO_2^+ velocities data (1–3), (1–3) and (1–2) $km\ s^{-1}$ [3-7,31]. The superthermal electron data for number density is (10^{10} – 10^{12}) m^{-3} and velocity (10 – 100) $km\ s^{-1}$ [8-9]. The following initial conditions for the self-similar solution which we used here indicate that every physical parameter preserves its shape during the expansion and there is no scaling parameter

$$\begin{aligned}
 N_O[0] &= 4, N_{O_2}[0] = 2, N_{CO_2}[0] = 1, N_e[0] = 5 \\
 V_O[0] &= 1, V_{O_2}[0] = 1, V_{CO_2}[0] = 1, V_e[0] = 6 \text{ and } \Phi[0] = 0.
 \end{aligned}$$

Note that the electrons possess low inertia and respond more quickly than positive ions to any disturbance. An ambipolar electrostatic field between both species will be generated causing the plasma to expand.

In Fig. (1), we present the dependence of the superthermality factor κ as a function of various properties of the expanding plasma: Fig. (1a) shows how the normalized number density of the O^+ ion, there is increased in the depletion of oxygen density for increasing κ , Fig. (1b) represents the variation of κ with the normalized velocity of the O^+ ions and reflects the fact that oxygen velocity is increased with the increase of κ . In Fig. (1c), electric potential due to superthermal electrons during the expansion is shown, which reflects that electric potential increases with an increase in higher values of κ . The negativity in electric potential is directly proportional to superthermality factor κ . It is clear from this that for higher values of superthermality the plasma expansion is larger compared to lower values. At higher values of κ , both the velocity and depletion enhance, which strengthens the electric potentials accelerating ions and further enhances plasma density depletion for an easy escape mechanism. Due to the high energy of superthermal electrons, they inhibit the ions from keeping up with their velocity. This results in the inability of the ions to accelerate fast enough to match the electron speed. At lower superthermality values, this leads to a reduction in the plasma expansion domain.

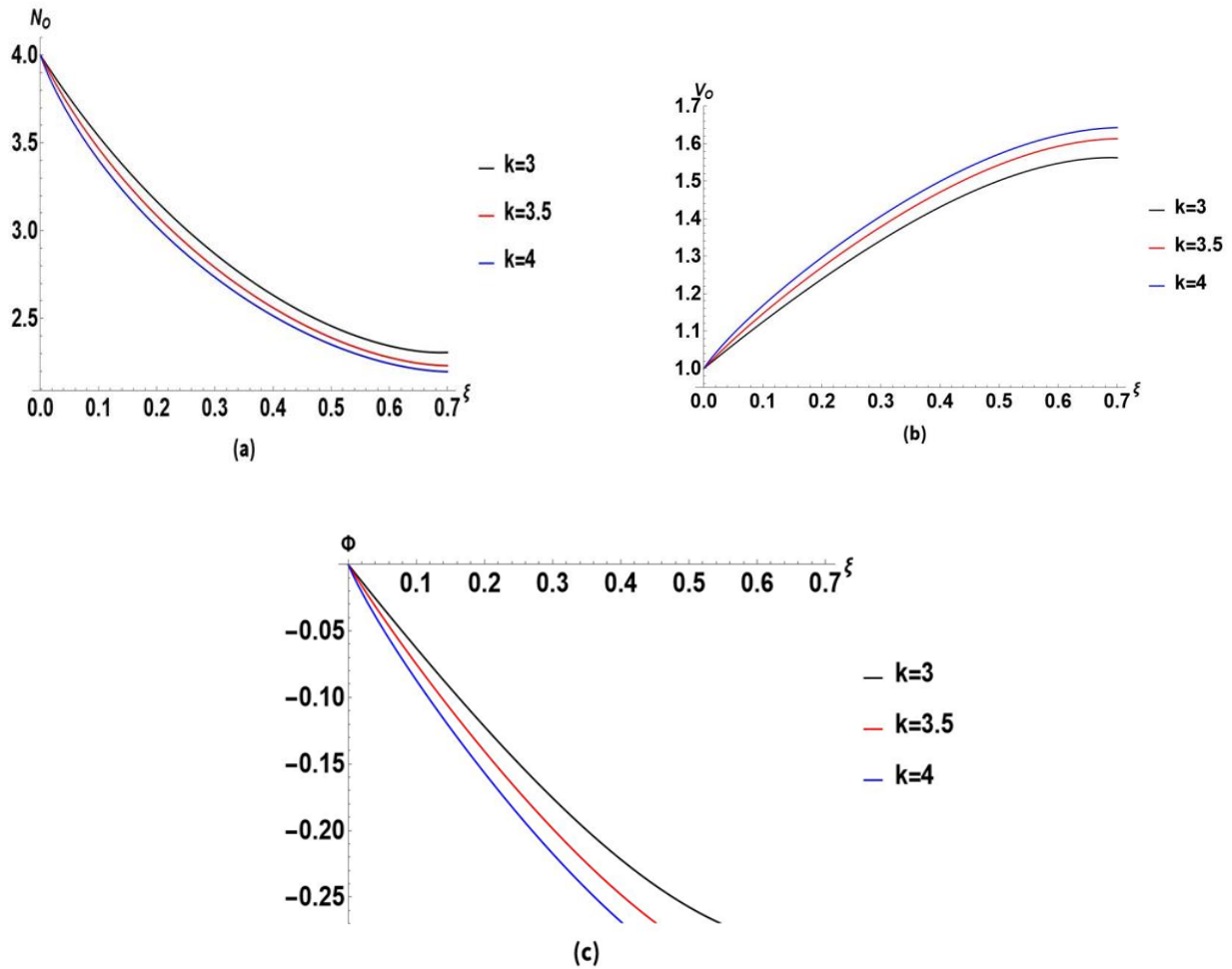


Fig.1: The normalized profiles of number density (a), velocity (b), and electric potential (c) versus self-similar variable ξ for O^+ for three values of superthermality factor κ .

In Fig. (2) we studied the effect of the initial oxygen density to initial electron density ratio $\beta = n_{O_0}/n_{e_0}$ on the normalized number density of the expanding plasma of O^+ ion in Fig. (2a), the impact of β on the normalized velocity of O^+ ion in Fig. (2b) and the electric potential generated during the expansion in Fig.(2c). In Fig. (2a) that the depletion in the oxygen density N_o decreases when increasing the initial oxygen to initial electron density ratio. The effect of initial oxygen to initial electron density ratio on the positive oxygen velocity V_o is shown in Fig. (2b). It is observed that the velocity of the oxygen ions decreases as β increases, and this change in β also influences the electric potential as shown in Fig. (2c), As β increases, the electric potential is less negative and hence reflects the reduced capacity of the plasma. For large ratios of oxygen to electron density, the density of oxygen ions increases, this facilitates recombination processes and reduces the density of free charge carriers. Weakened by the decrease in the population of charge carriers, the ambipolar electric field is a key mechanism for ion acceleration and expansion of plasma. A weaker ambipolar electric field reduces the plasma's capacity to sustain the forces necessary for effective ion acceleration. This is observed as reduced ion velocities, lower ion density depletion, and a constrained expansion region. The less negative electric potential is direct evidence of the reduced strength of the electric field. This indicates the system's incapacity to maintain the dynamic forces necessary for expansion. Consequently, it creates a regime where the plasma achieves both stability and confinement, effectively inhibiting any further expansion.

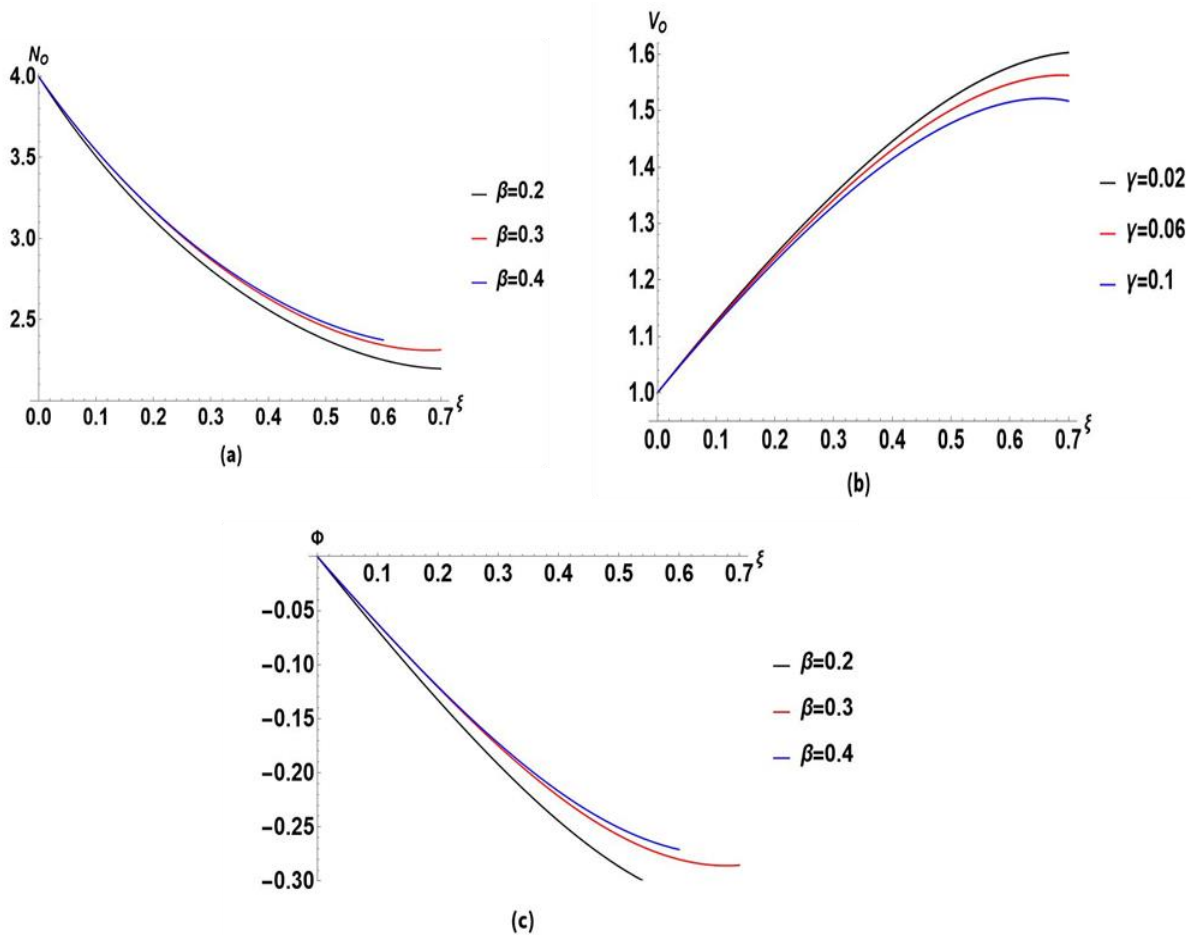


Fig.2: The normalized profiles of number density (a), velocity (b), and electric potential (c) versus self-similar variable ξ for O^+ for three values of β .

In Fig. (3), we examine the impact of the initial carbon dioxide to electron density ratio $\gamma = n_{CO_2_0}/n_{e_0}$ on the normalized number density of the expanding plasma of O^+ ion in Fig. (3a), the impact of γ on the normalized velocity of O^+ ion in Fig. (3b) We examine the electric potential established during the expansion in Fig. (3c), in Fig. (3a) that the depletion in the oxygen density N_O decreases when increasing the initial the carbon dioxide to initial electron density ratio. The effect of initial the carbon dioxide to initial electron density ratio on the positive oxygen velocity V_O is shown in Fig. (3b). It is evident that the oxygen velocity decreases with the increase of γ . The effect γ on the electric potential is shown in Fig. (3c). As γ increases, the electric potential becomes less negative, indicating a redistribution of energy within the plasma. The higher the ratio of carbon dioxide to electron density, the heavier the carbon dioxide ions become and start dominating, significantly decreasing the mobility of lighter ions like oxygen. A more massive plasma system with this high density of carbon dioxide ions experiences a redistribution of its electric potential energy among ions, thereby diminishing the strength of the ambipolar electric field mechanism crucial in driving ion acceleration and regulating the dynamics of a plasma. The weakening of this field is reflected in the decrease of oxygen ion velocities and a reduced ion depletion rate, which consequently results in a reduced plasma expansion domain. The less negative electric potential signifies the diminished capacity of the plasma to sustain the forces required for effective ion acceleration. These interconnected effects stabilize the plasma, causing it to enter a regime dominated by confinement and characterized by limited dynamical behavior.

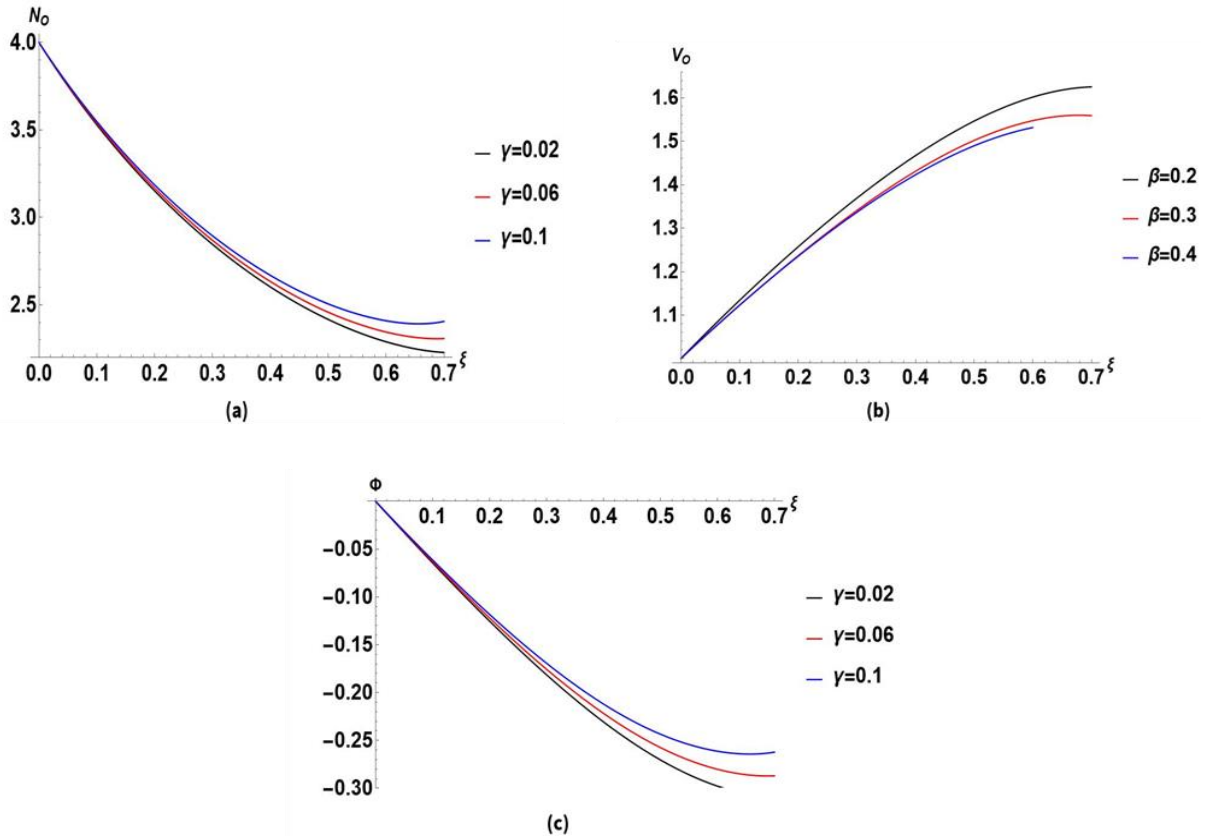


Fig.3: Profile of the normalized the number density (a), velocity (b), and electric potential (c) versus self-similar variable ξ for O^+ for three values of γ .

3. CONCLUSION

In this study, we conducted a detailed nonlinear numerical investigation to understand the impact of superthermal electron distributions on the lower ionosphere of Mars, specifically focusing on the key mechanisms governing their interactions. A plasma fluid model was employed to characterize the plasma environment in the ionosphere of Mars at altitudes between 200 and 350 km by adopting a self-similarity approach. The model equations were solved numerically, with initial conditions for different plasma variables based on observational data from MAVEN. The primary findings of the study are summarized as follows:

Superthermal electrons significantly influence the plasma expansion dynamics. Higher κ values enhance the ambipolar electric field, resulting in greater depletion of oxygen ions, increased ion velocities, and a more negative electric potential. This indicates that superthermal electrons, owing to their higher energy, amplify the plasma expansion by increasing charge separation and accelerating ionized species. The increased electric potential reflects the enhanced capacity of the plasma to overcome ion retention forces, thus facilitating ion escape from the ionosphere.

The initial oxygen-to-electron density ratio β plays a crucial role in modulating the effects of superthermal electrons. As β increases, oxygen ion depletion diminishes, ion velocities decrease, and the electric potential becomes less negative. This behavior arises because a higher β corresponds to a denser ion population relative to electrons, leading to reduced charge separation and weakening the ambipolar electric field. As a result, the reduced charge separation causes the plasma to retain more electrons, resulting in a weaker ambipolar electric field. This stabilizes the plasma by decreasing ion acceleration and reducing the spatial extent of plasma expansion.

The carbon dioxide-to-electron density ratio γ introduces a stabilizing effect due to the greater mass of carbon dioxide ions. As γ increases, the depletion of oxygen ions and their velocities decrease, while the electric potential weakens. Heavy ions like CO₂ dominate plasma dynamics by exerting a drag force on lighter oxygen ions and redistributing the energy of the ambipolar electric field. This redistribution weakens the field's ability to accelerate ions, resulting in a smaller plasma expansion domain as the system becomes less responsive to the energizing influence of superthermal electrons.

These findings reveal a complex interplay between electron energy distribution and ion composition in controlling plasma expansion and ion escape from Mars' ionosphere. Regions with high κ values, coupled with low β and γ , are more prone to ion escape due to stronger electric fields and enhanced ion acceleration. Conversely, areas with higher β and γ ratios act as stabilizing regions that retain ions and mitigate atmospheric loss.

This study underscores the critical roles of superthermal electrons, ion-to-electron density ratios, and heavy-ion effects in shaping the dynamics and evolution of the Martian ionosphere. These processes not only govern plasma behavior but also have significant implications for the long-term atmospheric escape rates and the planetary environment's stability.

4. REFERENCES

- [1] V. K. Yadav, "Plasma waves around Venus and Mars," *IETE Technical Review*, vol. 38, no. 6, pp. 622-661, 2021.
- [2] B. M. Jakosky, R. P. Lin, J. M. Grebowsky, J. G. Luhmann, D. F. Mitchell, G. Beutelschies, and R. Zurek, "The Mars atmosphere and volatile evolution (MAVEN) mission," *Space Sci. Rev.*, vol. 195, pp. 3-48, 2015.
- [3] S. Sakai, L. Andersson, T. E. Cravens, D. L. Mitchell, C. Mazelle, A. Rahmati, and B. M. Jakosky, "Electron energetics in the Martian dayside ionosphere: Model comparisons with MAVEN data," *J. Geophys. Res.: Space Phys.*, vol. 121, no. 7, pp. 7049-7066, 2016.
- [4] X. S. Wu, J. Cui, S. S. Xu, R. J. Lillis, R. V. Yelle, N. J. Edberg, and D. L. Mitchell, "The morphology of the topside Martian ionosphere: Implications on bulk ion flow," *J. Geophys. Res.: Planets*, vol. 124, pp. 734-751, 2019.
- [5] K. G. Hanley, J. P. Mcfadden, D. L. Mitchell, C. M. Fowler, S. W. Stone, R. V. Yelle, and B. M. Jakosky, "In situ measurements of thermal ion temperature in the Martian ionosphere," *J. Geophys. Res.: Space Phys.*, vol. 126, no. 12, e2021JA029531, 2021.
- [6] Y. Cao, J. Cui, W. Liang, X. Wu, and H. Lu, "Characteristic timescales for the dayside martian ionosphere: chemistry, diffusion, and magnetization," *Astron. J.*, vol. 166, no. 6, p. 264, 2023.
- [7] Y. Cao, J. Cui, W. Liang, X. Wu, and H. Lu, "Characteristic timescales for the dayside martian ionosphere: chemistry, diffusion, and magnetization," *Astron. J.*, vol. 166, no. 6, p. 264, 2023.
- [8] S. Xu, S. M. Curry, D. L. Mitchell, J. G. Luhmann, R. J. Lillis, and C. Dong, "Superthermal electron deposition on the Mars nightside during ICMEs," *J. Geophys. Res.: Space Phys.*, vol. 125, no. 10, e2020JA028430, 2020.

- [9] S. Xu and M. W. Liemohn, "Superthermal electron transport model for Mars," *Earth Space Sci.*, vol. 2, no. 3, pp. 47-64, 2015.
- [10] Q. Zhang, "Ion escape from Mars," Ph.D. dissertation, Umeå Univ., Umeå, Sweden, 2023.
- [11] P. Mora, "Plasma expansion into a vacuum," *Phys. Rev. Lett.*, vol. 90, p. 185002, 2003.
- [12] S. P. Christon, D. G. Mitchell, D. J. Williams, L. A. Frank, C. Y. Huang, and T. E. Eastman, "Energy spectra of plasma sheet ions and electrons from ~ 50 eV/e to ~ 1 MeV during plasma temperature transitions," *J. Geophys. Res.: Space Phys.*, vol. 93, no. A4, pp. 2562-2572, 1988.
- [13] V. Pierrard and J. Lemaire, "Lorentzian ion exosphere model," *J. Geophys. Res.: Space Phys.*, vol. 101, no. A4, pp. 7923-7934, 1996.
- [14] S. M. Krimigis, J. F. Carbary, E. P. Keath, T. P. Armstrong, L. J. Lanzerotti, and G. Gloeckler, "General characteristics of hot plasma and energetic particles in the Saturnian magnetosphere: Results from the Voyager spacecraft," *J. Geophys. Res.: Space Phys.*, vol. 88, no. A11, pp. 8871-8892, 1983.
- [15] T. K. Baluku and M. A. Hellberg, "Ion acoustic solitons in a plasma with two-temperature kappa-distributed electrons," *Physics of Plasmas*, vol. 19, 2012.
- [16] V. Pierrard and M. Lazar, "Kappa distributions: Theory and applications in space plasmas," *Solar Phys.*, vol. 267, pp. 153-174, 2010.
- [17] W. M. Moslem and A. S. El-Said, "Formation of surface nano-structures by plasma expansion induced by highly charged ions," *Physics of Plasmas*, vol. 19, no. 12, 2012.
- [18] I. S. Elkamash and I. Kourakis, "Multispecies plasma expansion into vacuum: The role of secondary ions and suprathermal electrons," *Phys. Rev. E*, vol. 94, no. 5, p. 053202, 2016.
- [19] S. Salem, W. M. Moslem, R. Sabry, M. Lazar, R. E. Tolba, and S. K. El-Labany, "Ion escape from the upper ionosphere of Titan triggered by the solar wind," *Astrophys. Space Sci.*, vol. 364, pp. 1-7, 2019.
- [20] S. Salem, W. M. Moslem, H. Fichtner, and M. Lazar, "Solar wind effect on the multi-fluid plasma expansion in the Venusian upper ionosphere," *Astron. Astrophys.*, vol. 685, A152, 2024.
- [21] S. M. F. Salem, R. Tolba, W. Moslem, and S. El-Labany, "The Role of Superthermal Electrons on the Escaping Ions from The Upper Atmosphere of Titan and Venus," *Alfarama J. Basic & Appl. Sci.*, vol. 2, no. 1, pp. 97-104, 2021.
- [22] M. Djebli, "Charge evolution in dusty plasma expansion with negative ions," *Physics of Plasmas*, vol. 10, no. 12, pp. 4910-4912, 2003.
- [23] M. Djebli, R. Annou, and T. H. Zerguini, "Nonideal dusty plasma expansion," *Physics of Plasmas*, vol. 11, no. 5, pp. 2267-2271, 2004.
- [24] S. K. El-Labany, H. N. Abd El-Razek, and G. A. El-Gamish, "Opposite polarity dusty plasma expansion in Earth's mesosphere," *Astrophys. Space Sci.*, vol. 353, pp. 413-416, 2014.
- [25] S. Salem, W. M. Moslem, M. Lazar, R. Sabry, R. E. Tolba, and R. Schlickeiser, "Ionospheric losses of Venus in the solar wind," *Adv. Space Res.*, vol. 65, no. 1, pp. 129-137, 2020.

- [26] D. Bennaceur-Doumaz, D. Bara, and M. Djebli, "Self-similar two-electron temperature plasma expansion into vacuum," *Laser Part. Beams*, vol. 33, no. 4, pp. 723-730, 2015.
- [27] M. Shahmansouri, A. Bemooni, and A. A. Mamun, "Self-similar expansion of adiabatic electronegative dusty plasma," *J. Plasma Phys.*, vol. 83, no. 6, 905830607, 2017.
- [28] W. M. Moslem, "Self-similar expansion of white dwarfs," *Astrophys. Space Sci.*, vol. 342, no. 2, pp. 351-355, 2012.
- [29] W. M. Moslem, A. S. El-Said, S. A. Morsi, R. Sabry, M. E. Yahia, S. K. El-Labany, and H. Bahlouli, "On the formation of nanostructures by inducing confined plasma expansion," *Results Phys.*, vol. 15, p. 102696, 2019.
- [30] A. S. El-Said, W. M. Moslem, and M. Djebli, "Surface nanostructuring by ion-induced localized plasma expansion in zinc oxide," *Appl. Phys. Lett.*, vol. 104, no. 23, 2014.
- [31] K. G. Hanley, C. M. Fowler, J. P. McFadden, D. L. Mitchell, and S. Curry, "MAVEN-STATIC observations of ion temperature and initial ion acceleration in the martian ionosphere," *Geophys. Res. Lett.*, vol. 49, no. 18, p. e2022GL100182, 2022.